Nuclear Engineering and Design 424 (2024) 113326

Contents lists available at ScienceDirect

Nuclear Engineering and Design

journal homepage: www.elsevier.com/locate/nucengdes

Verification of NODAL3 code with PWR MOX/UO_2 core transient benchmark

Surian Pinem [a,*], Wahid Luthfi [a], Peng Hong Liem [b,c]

[a] Research Center for Nuclear Reactor Technology, Research Organization for Nuclear Energy, National Research and Innovation Agency, Building 80th KST B.J. Habibie (PUSPIPTEK Serpong), South Tangerang, Banten 15310, Indonesia

[b] Cooperative Major in Nuclear Energy, Graduate School of Engineering, Tokyo City University (TCU), 1-28-1, Tamazutsumi, Setagaya, Tokyo, Japan

[c] Scientific Computational Division, Nippon Advanced Information Service, (NAIS Co., Inc.), 416 Muramatsu, Tokaimura, Ibaraki, Japan

ARTICLE INFO

Keywords:
NODAL3
PWR MOX/UO_2 transient benchmark
SRAC2006
Static and transient

ABSTRACT

This paper presents static and transient calculation results for the Pressurized Water Reactor (PWR) mixed oxide fuel (MOX)/UO_2 Core Transient Benchmark with a coupled neutronics thermal-hydraulics, multi-dimension, few-group neutron diffusion nodal code, NODAL3. The main purpose of this study was to determine the accuracy of the NODAL3 code in modeling certain conditions of the PWR core that use MOX fuel. In this work, cross-section data were generated with the PIJ module from the SRAC2006 code system (ENDF/B-VII.0 based library). Static parameters calculated cover multiplication factor, power distribution, control rod reactivity, and critical boron concentration. For transient cases, parameters to be verified were peak power time, maximum power, and final average Doppler temperature. The static parameter calculation results show good results when compared with DeCART reference solutions, with power-weighted error (PWE) and error-weighted error (EWE) less than 5 % on radial power distribution case. The differences in critical boron concentration from reference data on Hot Full Power (HFP) and Hot Zero Power (HZP) conditions were less than 30 ppm. The transient solution were in good agreement when compared to other codes.

1. Introduction

Research Organization for Nuclear Energy (ORTN) of National Research and Innovation Agency (BRIN) or previously known as National Nuclear Energy Agency of Indonesia (BATAN) was the only national Research and Development (R&D) institution in the nuclear field has carried out several planned and sustainable activities to support the national nuclear R&D program. In President Regulation of Republic Indonesia No. 22 of 2017 about General Plans for National Energy, the contribution of new and renewable energy was estimated to reach around 25 % and 31 % respectively in 2025 and 2050 (Yudiartono et al., 2018). Nuclear Power Plants (NPPs) as part of the new energy must be able to work together with renewable energy to replace fossil-based energy gradually, to support sustainable national development with better and clean energy.

Previously, BATAN has some experience in development of analytical tools for neutronics calculations. Several codes that have been developed by BATAN were 2-dimensional (2-D) and 3-dimensional (3-D) multigroup neutron diffusion codes, namely BATAN-2DIFF (Liem, 1994) and BATAN-3DIFF (Liem, 1999; Pinem and Sembiring, 2019) codes respectively. Verification and validation of these codes gives very satisfying results when compared to other codes and to the experimental data from the first criticality of the RSG-GAS multi-purpose reactor. In addition, an in-core fuel management code for research reactors has also been developed, i.e. the BATAN-FUEL code which has been used to establish the new equilibrium silicide core of the RSG-GAS reactor, and at present is being used for the reactor in-core management calculations (Liem, 1987; Pinem et al., 2016c). The 3-D coupled neutronic and thermal hydraulic calculation code, MTR-DYN (Pinem et al. 2009; Pinem et al. 2016a; Pinem et al., 2020), has also been developed for the RSG GAS and other plate-type (MTR type) research reactors to treat some important transient and accident scenarios, like the Reactivity Insertion Accident (RIA), reduced coolant flow rates, and several combined scenarios.

Based on the experiences and capacity building gained from the aforementioned code development, BATAN (*now* OTRN-BRIN) also conducting a similar effort for power reactors (light water reactors) called NODAL3. NODAL3 code can be used to solve either steady-state as

* Corresponding author.
E-mail address: suri001@brin.go.id (S. Pinem).

https://doi.org/10.1016/j.nucengdes.2024.113326
Received 14 September 2023; Received in revised form 5 February 2024; Accepted 18 May 2024
Available online 22 May 2024

well as time-dependent cases, by solving the few group neutron diffusion equations in 3-D Cartesian geometry and coupled with a simple thermal–hydraulic model for PWRs. Following the completion of the code, several verification steps were conducted. The NODAL3 code has been verified for calculating static and transient parameters on LWR benchmark cases and the results show a good agreement when compared to reference solutions (Sembiring and Pinem, 2012; Pinem et al., 2014, 2016b). This R&D effort has been focused on LWR type reactors because this type of reactor has higher feasibility of being built in Indonesia. Moreover, the local governments (provinces) increase their interest in small-medium size reactors (SMRs) because they can easily meet the needs of small-scale energy demand at an archipelago country like Indonesia. Several types of SMR were available while the LWR-based SMR was considered to have more mature technology so the NODAL3 code was then expected to contribute to this topic.

Another important issue for the future of large LWRs operations is the reliability of the uranium fuel supply. Regarding this issue and for other reasons, several countries have been pursuing the reprocessing option of spent fuel, recover the plutonium, manufacture, and use the MOX fuels for LWRs. By using MOX fuels, the use of uranium fuel can be reduced thus extending the lifetime of uranium resources. Other main advantages of using MOX fuels were reducing the amount of enriched uranium and reducing radioactive waste generated from spent nuclear fuel (Zheng et al., 2012). Although at present it is not clear whether the LWR to be built in Indonesia would use also MOX fuel, we considered the possibility and therefore we were motivated to step forward with the verification of the NODAL3 code against the MOX-fueled LWR core.

The purpose of this study is to verify NODAL3 performance in modeling the MOX-fueled core by using PWR MOX/UO_2 Core Transient Benchmark Problem (Kozlowski and Downar, 2006). This benchmark problem was released by the Nuclear Science Committee of the OECD Nuclear Energy Agency (NEA) which has been used as a reference by researchers/developers to verify their codes either in static or transient calculations. There are various challenges when dealing with mixed oxide (MOX) fuel LWR cores since the difference in fuel composition caused by the difference in burnup degree might affect core performance. Some of it came from the neutron spectrum hardening of MOX fuel containing fissile plutonium in comparison to typical UO_2 fresh fuel, making the neutron flux between each fuel assembly differ. This neutron gradient could affect neutron current solved by a typical diffusion solver which then needs a correction factor. Hence, proper calculation with a high degree of accuracy could be achieved for making correct decisions regarding core design, burn-up, and safety margins (Choe et al., 2019; Leppänen et al., 2014; Luthfi and Pinem, 2023). Coupled calculations between Monte Carlo code (Serpent 2) and thermal–hydraulic code (SUBCHANFLOW) were performed for the BEAVRS benchmark (Benchmark for Evaluation and Validation of Reactor Simulations) of MIT Computational Reactor Physics Group (CRPG) and also previously mentioned PWR MOX/UO_2 core transient benchmark (Daeubler et al., 2015; Ferraro et al., 2020).

In our previous works, the NODAL3 program was verified using the cross-section data provided within the PWR MOX/UO_2 Core Transient Benchmark data (Luthfi and Pinem, 2023). The lattice model solved using the collision probability method of PIC-SRAC with ENDF/B-VII.0 was used to generate cross-sections or group constants for NODAL3 which was then compared with cross-section provided by benchmark data that was generated by Purdue University using HELIOS v.1.8 with ENDF/B-VI nuclear data (Kozlowski and Downar, 2006). Another cross-section generated by Serpent2 Monte Carlo code and ENDF/B-VI.8 nuclear data (Imron and Hartanto, 2021), was also used to compare the NODAL3 performance, especially on its static benchmark cases. From this study, it was known that all cross-section data being used on NODAL3 shows a good agreement to data calculated with DeCART as a reference on control rod worth and static parameters, including critical boron concentration in HZP condition even with generated cross-section data by SRAC could differ for up to 80 % from HELIOS while Serpent differs for up to 19 % from HELIOS.

However, the capability to generate cross-sections for various reactors is essential, hence in this study, the cross-section data provided within the benchmark problem definition were not used. Instead, we improve our fuel assembly model on SRAC2006 code, i.e. fuel pin division and numerical integration parameters used in PIJ. SRAC2006 code has been widely used and shows good consistency in previous studies (Luthfi and Pinem, 2020). The SRAC2006 code (Okumura et al., 2007) was used to prepare the group constants (cross-section data) that used in the benchmark cases for both normal operation and rod ejection accident conditions. Calculation results related to steady-state and transient conditions from the NODAL3 code were compared with reference data from various codes that use either nodal or heterogeneous solutions (Kozlowski and Downar, 2006).

In next Chapter, a brief description of the PWR MOX/UO_2 Core Benchmark was given. The methodology adopted for group-constants preparation and NODAL3 calculation models are presented Methodology. The calculation results were then discussed in Result and Discussion, and finally, Conclusion gives the summary of the present work.

1.1. PWR MOX/UO_2 core benchmark

The reactor core selected for the benchmark was based on the Westinghouse PWR four-loop power plant, rated 3,565 MWth. This benchmark was mainly used to test the ability of reactor kinetic code to predict the steady-state and transient conditions of reactor core using UO_2/MOX fuel. The fuel assembly was 17 × 17, UO_2 fuel assembly with 104 Integral Fuel Burnable Absorber (IFBA) and MOX fuel assembly with 24 Wet Annular Burnable Absorber (WABA). Each MOX and UO_2 assembly have 2 different enrichments and configured to make a whole reactor core, as shown in the quarter-cores configuration in Fig. 1. The core was then surrounded by an axial (top–bottom) water reflector with a height equal to the pitch of the fuel assembly, and radially covered by water with an additional 2.52 cm of the baffle. The burn-up fraction of fuel assemblies also varies in the core.

Core design parameters could be seen in Table 1, while fuel assembly configurations of UO_2 and MOX fuel assemblies are shown in Fig. 2 and its heavy metal composition shown in Table 2. A complete description of the benchmark cases can be found in references (Kozlowski and Downar, 2006). The whole PWR MOX/ UO_2 Core Transient Benchmark cases could be divided into 4 parts, namely.

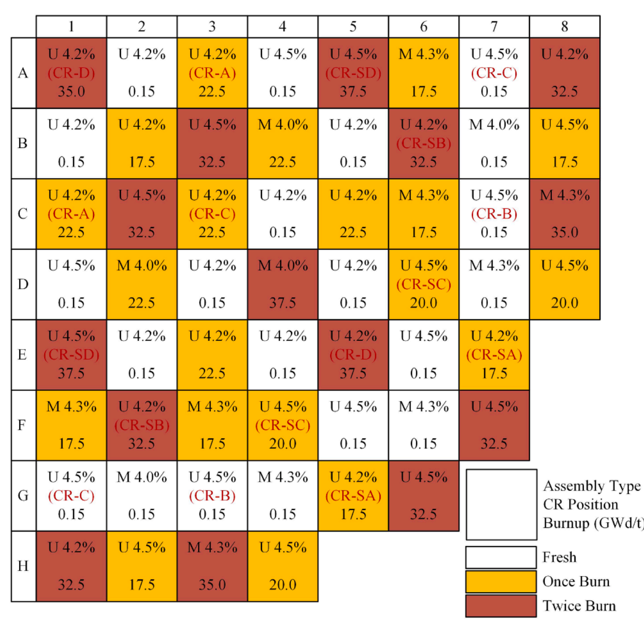

Fig. 1. Quarter-core configuration (Kozlowski and Downar, 2006).

Table 1
Core design parameters (Kozlowski and Downar, 2006).

Parameters	Value
Number of fuel assemblies	193
Power level (MWth)	3565
Core inlet pressure (MPa)	15.5
Hot Full Power (HFP) core average moderator temperature (K)	580
Hot Zero Power (HZP) core average moderator temperature (K)	560
Hot Full Power (HFP) core average fuel temperature (K)	900
Fuel lattice, fuel rods per assembly	17 × 17, 264
Number of control rod guide tubes	24
Number of instrumentation guide tubes	1
Total active core flow (kg/sec)	15849.4
Active fuel length (cm)	365.76
Assembly pitch (cm)	21.42
Pin pitch (cm)	1.26
Baffle thickness (cm)	2.52
Design radial pin-peaking (FH)	1.528
Design point-wise peaking (FQ)	2.5
Core loading (tHM)	81.6
Target cycle length (GWd/tHM) (months)	21.564 (18)
Capacity factor (%)	90
Target effective full power days	493
Target discharge burn-up (GWd/tHM)	40.0–50.0
Maximum pin burn-up (GWd/tHM)	62
Shutdown margin (SDM) (%Δρ)	1.3

1) Calculation of multiplication factor, rod worth, fuel assembly and pin power at 2-D Hot Zero Power (HZP) conditions,
2) Calculation of critical boron concentration, fuel assembly and pin power at 3-D Hot Full Power (HFP) conditions,
3) Calculation of critical boron concentration, fuel assembly and pin power at 3-D HZP conditions, and
4) Calculations of transient response to control rod ejection accident at 3-D HZP conditions.

The NODAL3 calculations results for all parts (Part 1–4) of the benchmark are presented on next section. However, since at the present state NODAL3 code cannot calculate pin power distribution within a fuel assembly, the calculation related to pin power was not presented in this study.

2. Methodology

All calculations of PWR MOX/UO_2 Core Transient Benchmark in 2-dimensional (2-D) and 3-dimensional (3-D) cases were carried out with the NODAL3 code, including static and transient parameters. Benchmark core consists of 193 fuel assemblies with size 21.42 cm × 21.42 cm, with 17 types of the fuel assembly and 8 of them have additional models to facilitate control rod insertion. The core was modeled in a symmetrical quarter core geometry with 2 × 2 nodes for each fuel assembly, radially, and 1 (one) node for each axial layer in 3-D models. The axial fuel zone of the reactor with a total height of 365.76 cm was divided into 16 layers, with a thickness of 22.86 cm and an additional 21.42 cm of water as an axial reflector on top and bottom of the fuel zone, a total of 18 axial layers. These node selections (axial and radial) were based on previous studies on the sensitivity of node size in geometry, the node in fuel pellet-cladding for heat transfer, also maximum time steps during the transient calculation of the NEACRP 3D LWR benchmark core (Pinem et al., 2016b).

NODAL3 code needs the macroscopic cross-sections (group constant) of core materials as a function of burnup, boron concentration, fuel temperature, moderator temperature related to moderator density, control rod conditions (inserted or withdrawn). The dependency of the group-constant set on the above-mentioned parameters was expressed in polynomial functions. This group-constant set was prepared by the commonly used base and branch procedure. The base group-constant set

Table 2
Heavy metal composition in fuel (Kozlowski and Downar, 2006).

Assembly Type	Density (g/cm^3)	HM Material	
UO_2 4.2 %	10.24	U-235: 4.2 wt%, U-238: 95.8 wt%	
UO_2 4.5 %	10.24	U-235: 4.5 wt%, U-238: 95.5 wt%	
		Pu-fissile (wt%)	Uranium vector:
MOX 4.0 %	10.41	Corner zone: 2.5 wt% Peripheral zone: 3.0 wt% Central zone: 4.5 wt%	234/235/236/238 = 0.002/0.2/0.001/99.797 wt% Plutonium vector: 239/240/241/242 = 93.6/5.9/0.4/0.1 wt%
MOX 4.3 %	10.41	Corner zone: 2.5 wt% Peripheral zone: 3.0 wt% Central zone: 5.0 wt%	

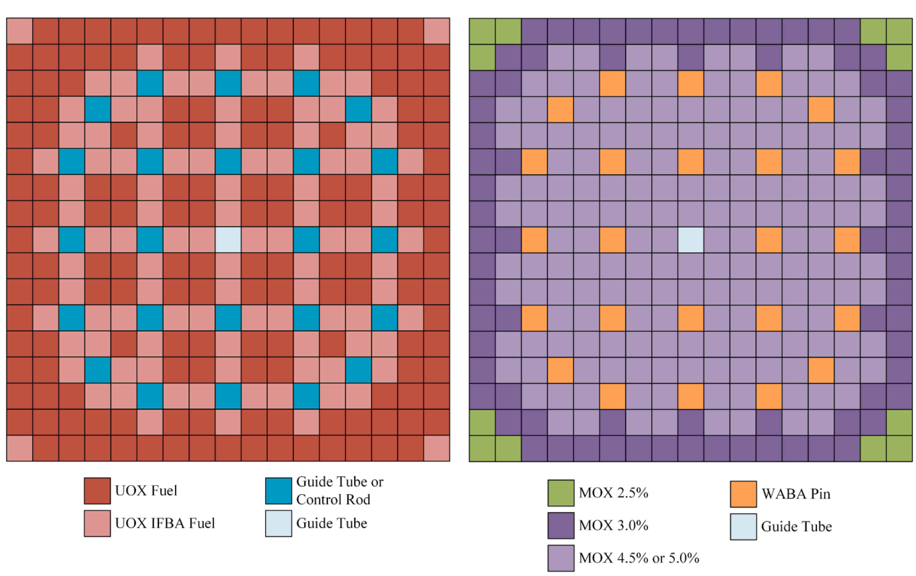

Fig. 2. UO2 fuel assembly with 104 IFBA pins and MOX fuel assembly with 24 WABA (Kozlowski and Downar, 2006).

was prepared using cell burnup calculations under the HFP condition. Then, the branch calculations for each parameter were conducted to obtain the polynomial function of the required group-constant format of NODAL3.

The above-mentioned cell-burnup calculations, the fuel assembly averaged macroscopic cross-sections of all types of fuel assembly were prepared by PIJ module in SRAC2006 code system using material composition provided by Purdue University (Purdue University, 2004). PIJ module was chosen because it has some options for detailed 2-D geometry of PWR fuel assembly to generate the cross-sections needed. PIJ module calculations use 107 energy groups (59 fast and 48 thermal neutron energy groups) of the ENDF/B-VII.0 nuclear data library. At the end of PIJ calculations, the obtained cross-sections were collapsed into 2 energy groups. Fuel assembly modeling within the PIJ module in the SRAC2006 system code was done by considering the detailed geometry data of the entire pin cell used in a fuel assembly. The size and material used in each type of fuel pin cell can be seen in Table 3. Each pin cell that has been modeled was then placed in a position that corresponds to each type of fuel assembly as shown in Fig. 2.

Since there were various types of fuel assembly used in the core benchmark, see Fig. 1, then each type of UO_2 and MOX fuel assembly at each level of enrichment, burnup degree, and control rod insertion that used in the core were modeled to obtain the required cross-section data (total of 25 types obtained from the base calculations). Then for transient calculations, branch calculations were conducted for the entire types of a fuel assembly according to the conditions shown in Table 4. Post-processing for all these calculations produces the required polynomial form of the NODAL3 group-constant set. Additionally, no Assembly Discontinuity Factors (ADF) were used in this calculation since the present version of NODAL3 was developed without ADF within its nodal diffusion solver. Besides, the PIJ module of SRAC2006 was not equipped with a solver to generate ADF, or it could be considered as a problem with ADF equal to 1. Hence, NODAL3 solves the neutron diffusion equation without additional correction of heterogeneous neutron population caused by heterogeneous fuel assembly used in the PWR MOX/UO_2 core benchmark.

3. Result and Discussion

To accurately describe error (deviation from reference data/solution) in radial power distribution, two metrics used for comparison of results were Power-Weighted Error (PWE) and Error-Weighted Error (EWE). Both were defined as a weighted average of the error by Eq. (1) and Eq. (2) respectively, and the assembly power relative error (%, percent), e_i, was defined by Eq. (3).

Table 3
Pin cell dimensions (cm) and materials (Kozlowski and Downar, 2006).

Cell type Radius	FP Fuel Pin	IFBA Integral Fuel Burnable Absorber	GT Guide Tube	CR Control Rod	WABA Wet Annular Burnable Absorber
r_1	0.3951	0.3951	0.5624	0.4331	0.2858
r_2	0.4010	0.3991	0.6032	0.4839	0.3531
r_3	0.4583	0.4010		0.5624	0.4039
r_4		0.4583		0.6032	0.4839
r_5					0.5624
r_6					0.6032
r_0-r_1	Fuel	Fuel	Water	CR	Water
r_1-r_2	Gap	IFBA	Clad	Clad	Clad
r_2-r_3	Clad	Gap		Water	WABA
r_3-r_4		Clad		Clad	Clad
r_4-r_5					Water
r_5-r_6					Clad

Table 4
Cross-section calculation conditions.

Parameters	ID	1	2	3	units
Moderator temperature		600	580	560	K
Moderator density	D	661.14	711.87	752.06	gr/L
Boron concentration	B	0	1000	2000	ppm
Fuel temperature	F	560	900	1320	K

$$PWE = \frac{\sum_i |e_i| ref_i}{\sum_i ref_i} \quad (1)$$

$$EWE = \frac{\sum_i |e_i||e_i|}{\sum_i |e_i|} \quad (2)$$

$$e_i = \frac{calc_i - ref_i}{ref_i} \times 100 \quad (3)$$

3.1. Multiplication factor, rod worth and assembly power with 2-D core model

The calculation results of NODAL3 for the 2-D case were presented in Table 5. The calculation results were compared with the high-order heterogeneous multi-group DeCART transport code as the reference data/solution. Based on the calculations in Table 5, it can be seen that the difference of total control rod worth is 49 pcm higher from DeCART. The difference in multiplication factor (keff) for All Rods Out (ARO) and All Rods In (ARI) were 527 pcm and 411 pcm, respectively. While for the assembly power distributions, PWE and EWE for both ARO and ARI were less than 5 %, slightly higher than other codes, except BARS on ARI condition. Nevertheless, the results of NODAL3 calculations for the total control rod worth and multiplication factor were in good agreement when compared to other nodal code solutions.

The single rod worth results at ARO and ARI conditions are shown in Tables 6 and 7, respectively. The only heterogeneous solution available was from BARS and at ARO condition, NODAL3 results were in good agreement with the heterogeneous solution BARS, where its difference up to 4 pcm at (A,1) and (A,3) positions. The maximum difference between NODAL3 and PARCS was around 10 pcm and occurs at position (C,3).

At ARI conditions the performance of NODAL3 compared to BARS was not as good as in ARO conditions but still acceptable. As it could be seen in Table 5, the total control rod worth of BARS also lower than DeCART, so in this section, we could compare the NODAL3 data to PARCS 2G. The maximum difference between the highest and the lowest rod worth was 78 pcm and occurs at position (C,3). However, control rod worth between NODAL3 and PARCS 2G were in good agreement, with the maximum difference of 13 pcm at position (A,1).

DeCART code was used as the reference data for comparing assembly power distributions. Radial power distributions calculated at ARO and ARI conditions are shown in Figs. 3 and 4, respectively. The first line as a reference is DeCART, the second line is NODAL3 while the third line is the relative error between NODAL3 calculations from DeCART. Fig. 3 shows that the calculation of NODAL3 at ARO conditions were in good agreement compared to the reference with maximum relative error of 5.85 % at position (A,1).

The radial power distribution at ARI conditions shows good agreement from DeCART, where the maximum difference was 7.767 % at the (E,7) and (E-5) positions. UO_2 fuel assembly in this position was a once burned assembly with 17.5 GWd/t burnup, surrounded by a fresh fuel assembly at top and left, a twice burned assembly at bottom and right so that when the surrounding CR-A and CR-C rods were inserted a large gradient of neutron flux occurs and an accurate solution was more difficult to obtain. The three fuel assemblies surrounding the (B,2) UO_2 fuel assembly also show a high deviation to DeCART reference data.

Table 5
Comparison of multiplication factor and assembly power with 2-D core model.

NODAL Code	Total control rod (pcm)	ARO			ARI		
		k_{eff}	PWE	EWE	keff	PWE	EWE
Nodal solutions							
NODAL3	6850	1.06379	2.42	3.46	0.99154	2.77	4.69
EPISODE	6849	1.06364	0.96	1.64	0.99142	1.66	2.16
NUREC	6850	1.06378	0.96	1.63	0.99153	1.64	2.16
PARCS 2G	6850	1.06379	0.96	1.63	0.99154	1.67	2.18
SKETCH-INS	6850	1.06379	0.97	1.67	0.99153	1.67	2.16
Heterogeneous solutions							
BARS	6745	1.05826	1.29	1.92	0.98775	3.92	10.30
DeCART	6801	1.05852	ref	ref	0.98743	ref	ref

Table 6
Rod worth at ARO (pcm) with 2-D core model.

Code	Control rod position									
	(A,1)	(A,3)	(A,5)	A,7	(B,6)	(C,3)	(C,7)	(D,6)	(E,5)	(E,7)
Nodal solutions										
NODAL3	162	138	88	52	66	113	48	64	60	26
EPISODE	165	134	–	53	70	123	51	69	64	27
NUREC	166	143	91	53	70	125	51	68	64	27
PARCS 2G	166	143	91	53	70	123	51	68	64	27
SKETCH-INS	166	143	91	53	70	123	51	68	64	27
Heterogeneous solutions										
BARS	166	139	87	49	66	117	49	66	63	27

Table 7
Rod worth at ARI (pcm) with 2-D core model.

Code	Control rod position									
	(A,1)	(A,3)	(A,5)	(A,7)	(B,6)	(C,3)	(C,7)	(D,6)	(E,5)	(E,7)
Nodal solutions										
NODAL3	−853	−878	−408	−61	−153	−1115	−81	−293	−254	−22
EPISODE	−843	−884	–	−59	−155	−1130	−81	−293	−253	−24
NUREC	−840	−880	−405	−56	−152	−1127	−78	−290	−249	−21
PARCS 2G	−840	−880	−405	−56	−152	−1127	−78	−290	−249	−21
SKETCH-INS	−840	−880	−405	−56	−152	−1127	−78	−290	−249	−21
Heterogeneous solutions										
BARS	−914	−921	−417	−44	−145	−1193	−68	−313	−268	−17

These differences in radial power distribution results may also be attributed to the different nuclear data libraries used by DeCART or PARCS (ENDF/B-VI from HELIOS v.1.8) and PIJ SRAC (ENDF/B-VII.0). This was observed from previous studies that cross-section data calculated by PIJ SRAC can be 80 % lower than HELIOS on reflector region but the similar deviation on power distribution was more of the problem with the absence of ADF on NODAL3 solver (Luthfi and Pinem, 2023). However, the NODAL3 with cross-section data generated by the PIJ module of SRAC was in good agreement with the reference data and other computer codes.

3.2. Critical boron concentration with 3-D core model

Verification of critical boron concentrations was carried out under HFP and HZP conditions. HFP condition was defined as 100 % nominal power with 560 K inlet coolant temperature and all control rods were in a withdrawn position. Calculation result was then compared with PARCS 2G for reference. The critical boron concentration and core average thermal-hydraulics parameters at HFP are shown in Table 8. The difference in critical boron concentrations reaches only 26 ppm, while the Doppler temperature was 2.52 % (21.1 K) lower than reference data. Moderator density and moderator temperature were close to reference data. Radial power distribution results are shown in Fig. 5 with the highest difference from reference was around 6.77 % at position (A, 1). In comparison to the previous calculation in 2020 using coupled Serpent2 and SUBCHANFLOW, NODAL3 results give a lower than 50 ppm on critical boron difference, while average fuel and coolant temperature differ for below 2 Kelvin. The critical boron concentration and core average thermal-hydraulics parameters at HFP are shown in Table 8 (Ferraro et al., 2020).

Under HZP condition, the power was set to 10–4 % nominal power, inlet temperature to 560 K, all control rod banks inserted but all shutdown rods were in withdraw position. The results of calculated critical boron concentration, delayed neutron fraction, and assembly power at HZP condition are shown in Table 9. In this case, DeCART solution was used as reference data. NODAL3 critical boron concentration shows a good result, with a difference of 23 ppm to reference data. Calculated radial and axial power distributions (fractions) are shown in Figs. 6 and 7, respectively. The highest difference between radial power fractions from DeCART was around 6.61 % occurred at position (B, 2). Calculated axial power fractions were in good agreement to DeCART and other nodal solutions.

	1	2	3	4	5	6	7	8
A	1.298	1.723	1.350	1.531	0.999	1.016	1.029	0.417
	1.374	1.735	1.418	1.525	1.035	1.032	0.997	0.413
	5.855	0.696	5.037	0.392	3.604	1.575	3.110	0.959
B	1.724	1.495	1.180	1.223	1.377	0.893	0.983	0.502
	1.735	1.563	1.245	1.277	1.349	0.918	0.978	0.491
	0.638	4.548	5.508	4.415	2.033	2.800	0.509	2.191
C	1.351	1.181	1.274	1.468	1.221	1.103	1.028	0.392
	1.418	1.245	1.325	1.446	1.247	1.114	0.991	0.393
	4.959	5.419	4.003	1.499	2.129	0.997	3.599	0.255
D	1.534	1.225	1.470	1.033	1.354	1.144	0.906	0.355
	1.525	1.277	1.446	1.076	1.308	1.143	0.892	0.341
	0.587	4.245	1.633	4.163	3.397	0.087	1.545	3.944
E	1.002	1.382	1.224	1.357	0.892	1.123	0.608	
	1.035	1.348	1.247	1.308	0.904	1.067	0.585	
	3.293	2.460	1.879	3.611	1.345	4.987	3.783	
F	1.022	0.899	1.108	1.148	1.126	0.768	0.290	
	1.032	0.917	1.114	1.142	1.067	0.754	0.281	
	0.978	2.002	0.542	0.523	5.240	1.823	3.103	
G	1.040	0.993	1.037	0.912	0.611	0.291		
	0.997	0.978	0.991	0.892	0.585	0.281		
	4.135	1.511	4.436	2.193	4.255	3.436		
H	0.424	0.510	0.398	0.359			NODAL3	
	0.413	0.491	0.393	0.340			DeCART	
	2.594	3.725	1.256	5.292			Error relative (%)	

Fig. 3. Normalized radial power distribution at ARO condition with 2-D core model.

	1	2	3	4	5	6	7	8
A	1.150	2.423	1.176	2.188	0.744	0.653	0.320	0.208
	1.209	2.533	1.202	2.196	0.742	0.669	0.300	0.205
	5.130	4.540	2.211	0.366	0.269	2.450	6.250	1.442
B	2.423	2.288	1.695	2.032	1.884	0.458	0.490	0.274
	2.533	2.459	1.812	2.103	1.832	0.449	0.489	0.268
	4.540	7.474	6.903	3.494	2.760	1.965	0.204	2.190
C	1.176	1.695	1.201	2.555	1.949	0.966	0.349	0.201
	1.202	1.812	1.198	2.452	1.944	0.985	0.329	0.198
	2.211	6.903	0.250	4.031	0.257	1.967	5.731	1.493
D	2.189	2.033	2.555	1.795	1.744	0.553	0.457	0.192
	2.196	2.103	2.452	1.823	1.675	0.531	0.450	0.186
	0.320	3.443	4.031	1.560	3.956	3.978	1.532	3.125
E	0.744	1.885	1.950	1.745	0.513	0.729	0.206	
	0.742	1.832	1.944	1.675	0.508	0.696	0.190	
	0.269	2.812	0.308	4.011	0.975	4.527	7.767	
F	0.654	0.458	0.967	0.554	0.729	0.574	0.193	
	0.669	0.449	0.985	0.531	0.696	0.562	0.186	
	2.294	1.965	1.861	4.152	4.527	2.091	3.627	
G	0.322	0.493	0.351	0.459	0.206	0.193		
	0.300	0.489	0.329	0.450	0.190	0.186		
	6.832	0.811	6.268	1.961	7.767	3.627		
H	0.211	0.277	0.204	0.194			NODAL3	
	0.205	0.268	0.198	0.186			DeCART	
	2.844	3.249	2.941	4.124			Error relative (%)	

Fig. 4. Normalized radial power distribution at ARI condition with 2-D core model.

As previously shown in Fig. 3–Fig. 6, it could be seen that some positions of fuel assembly have a substantially high deviation to reference data within a range of 5–8 %, either on the core peripherals close to the radial water reflector or in the center of the core. This could be rooted in the absence of Assembly Discontinuity Factors (ADF) in NODAL3 so the heterogenous fuel assembly configuration of this benchmark core could not be solved accurately. It could be seen that on the core peripherals, ADF was important to solving severe neutron flux gradient on each node that was in contact with the water reflector. On the other hand, neutron diffusion calculation on low burnup UO_2 fuel close to the core center, in contact with high burnup UO_2 fuel or MOX

	1	2	3	4	5	6	7	8
A	1.023	1.388	1.143	1.398	0.964	1.101	1.159	0.467
	1.092	1.370	1.187	1.367	1.014	1.117	1.118	0.486
	6.774	1.282	3.876	2.189	5.176	1.471	3.572	4.090
B	1.388	1.217	1.010	1.149	1.335	0.937	1.135	0.570
	1.370	1.252	1.070	1.197	1.301	0.973	1.115	0.580
	1.282	2.884	5.901	4.143	2.539	3.842	1.771	1.667
C	1.145	1.011	1.125	1.358	1.190	1.192	1.154	0.457
	1.187	1.070	1.169	1.334	1.209	1.193	1.112	0.485
	3.694	5.796	3.867	1.738	1.597	0.042	3.605	6.039
D	1.402	1.152	1.360	1.004	1.333	1.192	1.032	0.396
	1.367	1.197	1.334	1.066	1.289	1.180	1.006	0.402
	2.468	3.872	1.882	6.135	3.278	1.040	2.558	1.389
E	0.968	1.341	1.194	1.337	0.895	1.177	0.653	
	1.014	1.301	1.209	1.289	0.932	1.123	0.645	
	4.742	2.975	1.256	3.568	4.089	4.596	1.286	
F	1.110	0.945	1.200	1.199	1.181	0.856	0.311	
	1.117	0.973	1.192	1.180	1.123	0.841	0.319	
	0.649	2.952	0.633	1.618	4.920	1.764	2.412	
G	1.175	1.150	1.167	1.042	0.657	0.310		
	1.118	1.115	1.112	1.006	0.645	0.319		
	4.885	3.052	4.687	3.493	1.887	2.742		
H	0.469	0.573	0.461	0.401			NODAL3	
	0.486	0.580	0.485	0.402			PARCS	
	3.646	1.134	5.119	0.125			Error relative (%)	

Fig. 5. Normalized radial power distribution for HFP with 3-D core model.

Table 9
Critical boron concentration at HZP with 3-D core model.

Code	Critical boron conc. (ppm)	Delayed neutron fraction (ppm)	Assembly power error	
			PWE	EWE
Nodal solutions				
NODAL3	1288	579	2.43	3.82
EPISODE	1340	579	1.05	3.42
NUREC	1343	576	1.05	3.43
PARCS 2G	1341	579	1.05	3.49
SKETCH-INS	1341	579	1.06	3.77
Heterogeneous solutions				
BARS	1296	579	2.65	5.66
DeCART	1265	–	ref	ref

Table 8
Critical boron concentration and core average thermal-hydraulics parameters at HFP with 3-D core model.

Code	Critical boron Conc. (ppm)	Assembly power error		Core average T/H properties		
		PWE	EWE	Doppler Temp. (K)	Moderator density (kg/m^3)	Moderator Temp. (K)
NODAL3	1653	3.00	3.82	815.2	707.0	580.1
EPISODE	1661	0.40	0.64	846.5	701.8	582.6
NUREC	1683	0.31	0.44	827.8	706.1	581.1
PARCS 2G	1679	ref	ref	836.0	706.1	581.3
SKETCH-INS	1675	1.04	1.39	836.6	705.5	580.9
Serpent-SUBCHANFLOW	1615	1.30	2.20	819.0	703.7	582.1

	1	2	3	4	5	6	7	8
A	0.366	0.813	0.546	1.564	1.290	1.147	0.523	0.276
	0.385	0.847	0.542	1.510	1.296	1.160	0.496	0.293
	5.191	4.182	0.733	3.453	0.465	1.133	5.163	6.159
B	0.813	0.817	0.778	1.340	1.822	1.048	0.806	0.373
	0.847	0.871	0.823	1.357	1.733	1.073	0.831	0.392
	4.182	6.610	5.784	1.269	4.885	2.385	3.102	5.094
C	0.547	0.778	0.647	1.612	1.630	1.324	0.591	0.307
	0.542	0.823	0.633	1.563	1.631	1.342	0.557	0.324
	0.914	5.784	2.164	3.040	0.061	1.360	5.753	5.537
D	1.565	1.341	1.612	1.262	1.666	1.441	1.032	0.363
	1.510	1.357	1.563	1.297	1.615	1.462	1.050	0.373
	3.514	1.193	3.040	2.773	3.061	1.457	1.744	2.755
E	1.291	1.823	1.631	1.666	0.643	1.395	0.822	
	1.296	1.733	1.631	1.615	0.633	1.367	0.824	
	0.387	4.937	0.000	3.061	1.555	2.007	0.243	
F	1.148	1.049	1.325	1.442	1.395	1.076	0.416	
	1.160	1.073	1.342	1.462	1.367	1.089	0.427	
	0.496	0.831	0.557	1.050	0.824	0.427	2.644	
G	0.525	0.807	0.592	1.033	0.823	0.417		
	0.496	0.831	0.557	1.050	0.824	0.427		
	5.524	2.974	5.912	1.646	0.122	2.398		
H	0.278	0.375	0.309	0.364			NODAL3	
	0.293	0.392	0.324	0.373			DeCART	
	5.396	4.533	4.854	2.473			Error relative (%)	

Fig. 6. Normalized radial power distribution for HZP with 3-D core model.

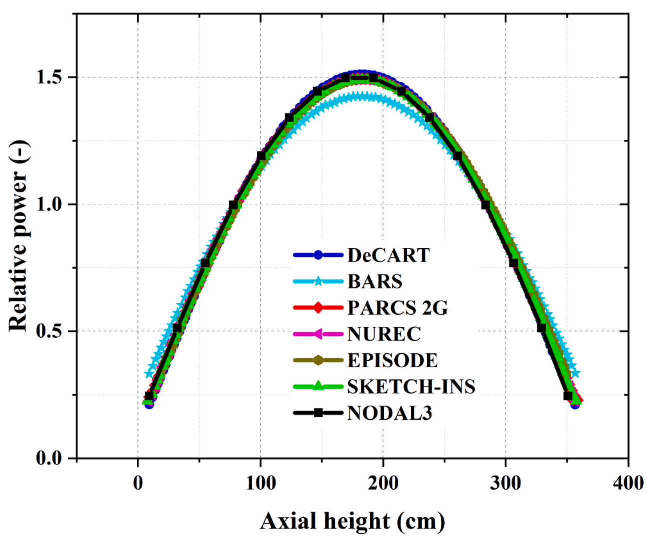

Fig. 7. Normalized axial power distribution at HZP with 3-D core model.

fuel can also affect calculated power distribution.

3.3. Transient with 3-D core model

The initial condition for the transient was in the HZP condition with 3-D core model where the core power was 10^{-4}% nominal power, inlet temperature 560 K, inlet pressure 15.5 MPa, all control banks inserted, and all shutdown banks out. The control rod ejection scenario was then modeled by pulling a single control rod in position (E-5) (cf. Fig. 1). The control rod was assumed to be fully ejected in 0.1 s without scram. During the calculation, boron concentration and other control rod positions were assumed to be constant and all transient parameters were calculated for the first 1.0 s. Calculated results then compared with available results from other codes.

The comparison of peak time, peak power, peak reactivity, and power integral are shown in Table 10. The result of NODAL3 calculations for peak power were in good agreement with PARCS 2G, and the highest deviation was 9.6 % when compared to EPISODE. As for the peak time, peak reactivity, and power integral, there was no significant difference from other nodal solutions. Nevertheless, in the heterogeneous solutions, results from BARS show a significant difference compared to other nodal solutions code.

Table 10
Peak time, peak power, peak reactivity and power integral of transient calculation.

Code	Peak time (s)	Peak power (%)	Peak Reactivity ($)	Power integral (% s)
Nodal solutions				
NODAL3	0.34	146	1.11	29.1
EPISODE	0.33	160	1.13	26.9
NEUREC	0.36	139	–	28.4
PARCS 2G	0.34	142	1.12	27.2
SKETCH-INS	0.34	144	1.12	28.0
Heterogeneous solutions				
BARS	0.21	522	1.29	41.7

The NODAL3 calculated results of transient core power and reactivity are shown in Figs. 8 and 9, respectively. In general, it shows a similar trend of transient core power and reactor reactivity compared to PARCS 2G and SKETCH-INS. NODAL3 reaches a maximum power of 146 % at 0.34 s, PARCS 2G reaches a maximum power of 142 % at 0.34 s, while SKETCH-INS reaches a maximum power of 144 % at 0.34 s. NODAL3 calculated maximum power was very close to PARCS 2G and SKETCH-INS with a difference of 2.7 % and 1.1 %, respectively.

Core average centerline fuel temperature (Doppler temperature) profile for NODAL3, PARCS 2G, and SKETCH-INS are shown in Fig. 10 and all results do not show any significant difference to each other at the beginning of transient as well as at near the end of the first 1.0 s. But at 0.3–0.6 s, NODAL3 gives a slightly lower temperature compared to PARCS 2G and SKETCH-INS. But temperature rising trends were in good agreement between NODAL3 and the other two codes, where it was initially constant and begins to increase gradually once the core power and reactivity start to change. Qualitatively the differences shown by NODAL3 may originate from different cross-section libraries used that may yield slightly different temperature and density feedback reactivity coefficients. Another factor which may also contribute was the thermal–hydraulic modeling of NODAL3 and its thermal property libraries (mostly steam thermal properties).

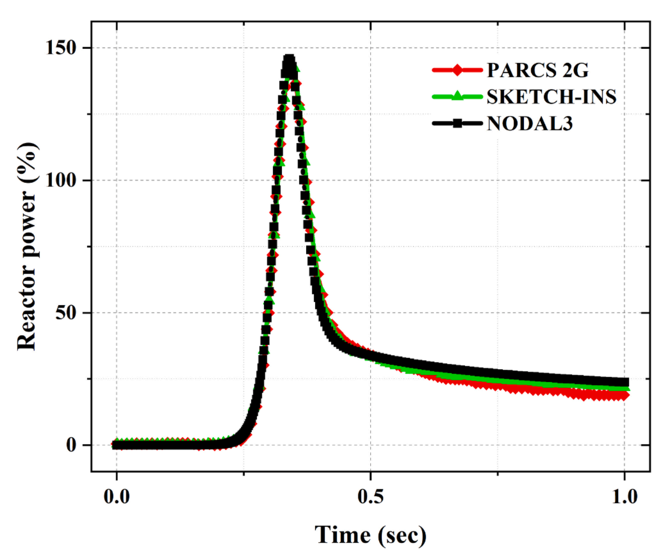

Fig. 8. Transient core power.

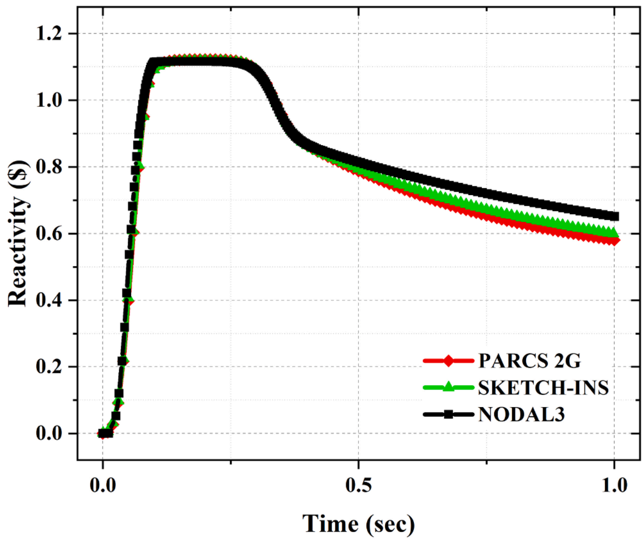

Fig. 9. Transient core reactivity.

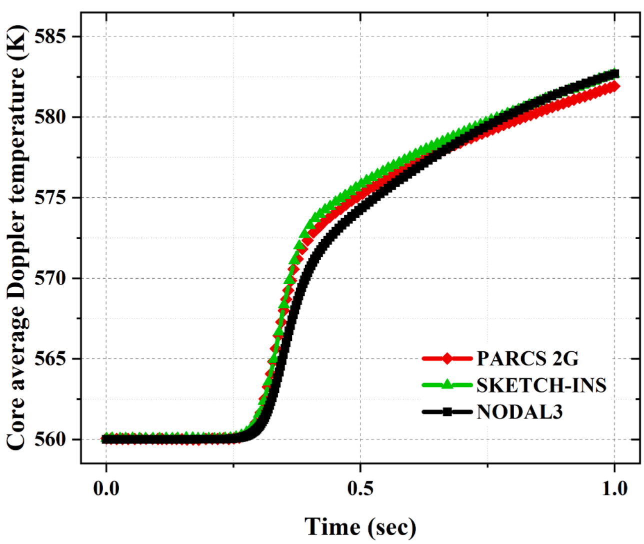

Fig. 10. Transient core average Doppler temperature.

4. Conclusion

PWR MOX/UO_2 Core Transient Benchmark calculations have been conducted using a coupled neutronics thermal-hydraulics, few-group, multidimensional nodal diffusion code, NODAL3 combined with the use of cross-section data generated by PIJ module of SRAC2006 Code System (ENDF/B-VII based library). The results of static calculations show that NODAL3 were in good agreement to DeCART reference data, with PWE and EWE of less than 5 %. The difference between the critical boron concentrations under HFP and HZP conditions does not exceed 26 ppm and 23 ppm from the reference data. While in transient calculation, NODAL3 also shows consistency to PARCS 2G and SKETCH-INS in core power, reactivity, and core average Doppler temperature profile. The maximum power calculated by NODAL3 has a difference of less than 3 % to PARCS 2G and 1 % to SKETCH-INS. As a conclusion, the results of NODAL3 static and transient calculations provide a good agreement in trend and consistency to reference data. NODAL3 needs to facilitate the use of ADF so it can improve its capabilities in modeling a heterogenous core configuration and enhance its consistency on calculated neutron flux (power) near core boundaries.

CRediT authorship contribution statement

Surian Pinem: Conceptualization, Data curation, Formal analysis, Funding acquisition, Methodology, Software, Validation, Writing – original draft, Writing – review & editing. **Wahid Luthfi:** Formal analysis, Methodology, Software, Validation, Visualization, Writing – original draft, Writing – review & editing. **Peng Hong Liem:** Conceptualization, Formal analysis, Methodology, Validation, Writing – review & editing.

Declaration of competing interest

The authors declare that they have no known competing financial interests or personal relationships that could have appeared to influence the work reported in this paper.

Data availability

No data was used for the research described in the article.

Acknowledgment

Thank you to the head of Research Center for Nuclear Reactor Technology (PRTRN) Research Organization for Nuclear Energy of National Research and Innovation Agency (ORTN-BRIN) for supporting this research.

References

Choe, J., Choi, S., Zhang, P., Park, J., Kim, W., Shin, H.C., Lee, H.S., Jung, J.E., Lee, D., 2019. Verification and validation of STREAM/RAST-K for PWR analysis. Nucl. Eng. Technol. 51 (2), 356–368. https://doi.org/10.1016/j.net.2018.10.004.

Daeubler, M., Ivanov, A., Sjenitzer, B.L., Sanchez, V., Stieglitz, R., Macian-Juan, R., 2015. High-fidelity coupled Monte Carlo neutron transport and thermal-hydraulic simulations using serpent 2/SUBCHANFLOW. Ann. Nucl. Energy 83, 352–375. https://doi.org/10.1016/j.anucene.2015.03.040.

Ferraro, D., Valtavirta, V., García, M., Imke, U., Tuominen, R., Leppänen, J., Sanchez-Espinoza, V., 2020. OECD/NRC PWR MOX/UO2 core transient benchmark pin-by-pin solutions using serpent/SUBCHANFLOW. Ann. Nucl. Energy 147, 107745. https://doi.org/10.1016/j.anucene.2020.107745.

Imron, M., Hartanto, D., 2021. Pressurized water reactor mixed oxide/UO2 transient benchmark calculations using Monte Carlo Serpent 2 Code and open nodal core simulator ADPRES. J. Nucl. Eng. Radiat. Sci. 7 (3), 1–8. https://doi.org/10.1115/1.4048764.

Kozlowski, T., Downar, T.J., 2006. Pressurised Water Reactor MOX/UO2 Core Transient Benchmark Final Report. OECD NEA Nuclear Science Committee Working Party on Scientific Issues of Reactor Systems: Nuclear Energy Agency, Organization for Economic Co-operation and Development.

Leppänen, J., Mattila, R., Pusa, M., 2014. Validation of the Serpent-ARES code sequence using the MIT BEAVRS benchmark - initial core at HZP conditions. Ann. Nucl. Energy 69, 212–225. https://doi.org/10.1016/j.anucene.2014.02.014.

Liem, P.H., 1994. Development and verification of Batan's standard, two-dimensional multigroup neutron diffusion code. Atom Indonesia 20 (1), 1–19.

Liem, P.H., 1999. Validation of BATAN'S standard 3-D diffusion code, BATAN-3DIFF, on the First core of RSG GAS. Atom Indonesia 25 (1), 47–53.

Liem, P. H. 1987. Batan-Fuel: A general in-core fuel management code. *Atom Indonesia* 22 (January 1996): 67–80.

Luthfi, W., Pinem, S., 2020. Calculation of 2-dimensional PWR MOX/UO2 core benchmark OECD NEA 6048 with SRAC code. J. Teknol. Reakt. Nukl. Tri Dasa Mega 22 (3), 89. https://doi.org/10.17146/tdm.2020.22.3.5955.

Luthfi, W., Pinem, S., 2023. Effect of cross-sections data on calculated static neutronic parameters of Pwr Mox/Uo2 core transient benchmark case using Nodal3 code. Acta Polytechnica 63 (4), 242–1229. https://doi.org/10.14311/AP.2023.63.0242.

Okumura, K., Kugo, T., Kaneko, K., Tsuchihashi, J., 2007. SRAC2006: A Comprehensive Neutronics Calculation Code System. Japan Atomic Energy Agency, Tokai.

Pinem, S., Liem, P.H., Sembiring, T.M., Surbakti, T., 2016a. Fuel element burnup measurements for the equilibrium LEU silicide RSG GAS (MPR-30) core under a new fuel management strategy. Ann. Nucl. Energy 98. https://doi.org/10.1016/j.anucene.2016.08.010.

Pinem, S., Sembiring, T.M., 2019. Accuracy of Batan-3DIFF and MCNP6 codes for thermal neutron flux distribution at the irradiation position of RSG-GAS reactor. Int. J. Nucl. Energy Sci. Technol. 13 (4), 295–312. https://doi.org/10.1504/IJNEST.2019.106050.

Pinem, S., Sembiring, T.M., Setiyanto, 2009. Transient analysis of RSG-GAS reactor core for coolant flow reduction using MTR-DYN Code. Tri Dasa Mega 11 (3), 153–161.

Pinem, S., Sembiring, T.M., Liem, P.H., 2014. The verification of coupled neutronics thermal-hydraulics code NODAL3 in the PWR rod ejection benchmark. Sci. Technol. Nucl. Install. 1–9. https://doi.org/10.1155/2014/845832.

Pinem, S., Sembiring, T.M., Liem, P.H., 2016b. Neutronic and thermal-hydraulic safety analysis for the optimization of the uranium foil target in the RSG-GAS reactor. Atom Indonesia 42 (3), 123–1118.

Pinem, S., Sembiring, T.M., Liem, P.H., 2016c. NODAL3 sensitivity analysis for NEACRP 3D LWR core transient benchmark (PWR). Sci. Technol. Nucl. Install. 1–11. https://doi.org/10.1155/2016/7538681.

Pinem, S., Sembiring, T.M., Surbakti, T., 2020. Reactivity insertion accident analysis during uranium foil target irradiation in the RSG-GAS reactor core. Nucl. Technol. Radiat. Protect. 35 (3), 1–7.

Purdue University. 2004. OECD/NEA AND U.S. NRC PWR MOX/UO2 CORE TRANSIENT BENCHMARK. 2004. https://engineering.purdue.edu/PARCS/MOX_Benchmark.

Sembiring, T.M., Pinem, S., 2012. The validation of the NODAL3 code for static cases of the PWR benchmark core. J. Nucl. Sci. Technol. Ganendra 15 (2), 82–92.

Yudiartono, A., Sugiyono, A., Wahid, L.M.A., Adiarso, 2018. Outlook energy Indonesia 2018. Pusat Pengajian Industri Proses Energi 53.

Zheng, Y., Hongchun, Wu., Cao, L., Jia, S., 2012. Economic evaluation on the MOX fuel in the closed fuel cycle. Sci. Technol. Nucl. Install. https://doi.org/10.1155/2012/698019.